ACS OMEGA

http://pubs.acs.org/journal/acsodf

Article

Improved Aluminum Adjuvants Eliciting Stronger Immune Response When Mixed with Hepatitis B Virus Surface Antigens

Zhibiao Wang, Shuxiang Li, Pu Shan, Duoqian Wei, Shaojie Hao, Zhuan Zhang, and Jing Xu*

Cite This: *ACS Omega* 2022, 7, 34528−34537

Read Online

ACCESS | Metrics & More | Article Recommendations

ABSTRACT: Adjuvants can regulate the immune response triggered by vaccines. Traditional aluminum adjuvants can induce humoral immunity, but they lack the ability to effectively induce Th1 cellular immunity, which is not conducive to the development of vaccines with improved protective effects. Aluminum adjuvants from different sources may have different physicochemical properties, and therefore, completely different immune responses can be triggered. This suggests that adjuvant recognition by the immune system and its responses are closely associated with the physicochemical properties of the adjuvant itself. To test this hypothesis, in this study, we developed a new method for preparing an aluminum adjuvant. This aluminum adjuvant has a pseudoboehmite structure, strong protein adsorption capacity, and excellent suspension stability. The adjuvant was tested using the hepatitis B virus surface antigen (HBsAg) as a model antigen for immunization; the results showed that this aluminum adjuvant effectively induced not only humoral immunity but also an outstanding cellular immune response. These results provide a reference for improving the efficacy of adjuvants.

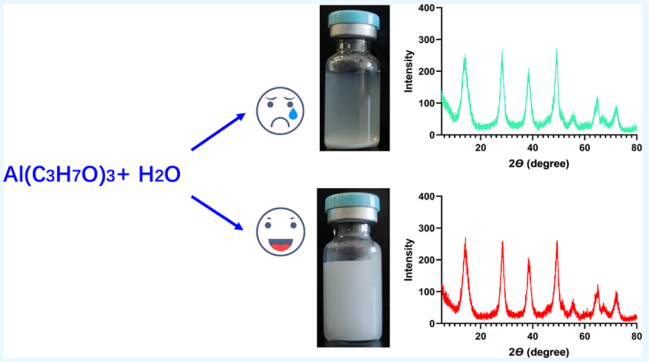

INTRODUCTION

Aluminum adjuvants have been used for nearly a century since they were first included in a vaccine in 1926.[1] As the most widely used vaccine adjuvants that have been used in the largest number of vaccines in history, aluminum adjuvants have been proven safe and effective. It is generally believed that aluminum adjuvants can effectively adsorb antigens and that depot formation occurs after they enter the body. These depots are thought to slowly release antigens to provide a long-lasting immune response. Furthermore, adjuvants can induce free antigens to aggregate into particles, resulting in improved uptake of antigens by antigen-presenting cells.[2] Adjuvants also protect antigens from being degraded and improve their stability.[3] They activate NLRP3, caspase-1, and other targets to induce the production of danger signals, thereby promoting the secretion of IL-1β, IL-18, and other cytokines.[4,5] However, aluminum adjuvants also have certain limitations. The poor induction of Th1 cellular immunity means that it is difficult to remove pathogens that have entered cells, resulting in an inability to prevent some diseases (such as AIDS and malaria). Thus, developing aluminum adjuvants that can induce superior Th1 cellular immunity is of great significance.

Although aluminum salts have been used as adjuvants for nearly a century, questions remain about the exact nature of their mechanism of action, and the results of some studies appear to be contradictory. For example, many studies have shown that the efficacy of an aluminum adjuvant is not related to its slow release of the antigen.[6,7] This could be because the aluminum adjuvant itself is not a single compound; similar to the delivery system, it has a complex structure. Thus, aluminum adjuvants obtained from different sources or via different preparation methods may be completely different; their mechanism of action may also be different, and they may induce different immune responses. The differences in the responses of the immune system to different exogenous substances (such as adjuvants) are related not only to the biological properties of the substances but also to their physical and chemical properties,[8] including surface morphology, charge, particle size, and even the hardness and optical rotation of materials.[9] This suggests the possibility of developing aluminum adjuvants with different physical and chemical properties by modifying the preparation method. Aluminum salts with improved or different adjuvant properties may thus be obtained.

Pseudoboehmite is a crystalline form of aluminum with chemical formula AlOOH. It has an amorphous or irregular

Received: July 6, 2022
Accepted: September 8, 2022
Published: September 15, 2022

https://doi.org/10.1021/acsomega.2c04266
ACS Omega 2022, 7, 34528−34537

crystal structure and a larger specific surface area than other crystal forms of AlOOH, which means that it may have a better adsorption capacity for antigens. Boehmite and pseudoboehmite have similar X-ray diffraction (XRD) patterns, but the diffraction peak of pseudoboehmite is wider than that of boehmite.[10] Thus, pseudoboehmite can be regarded as poorly crystallized boehmite.

Boehmite (or pseudoboehmite) can be prepared via a range of methods, including electrochemical,[11] gas phase precipitation,[12] microemulsion,[13] and hydrothermal methods.[14] Among these, hydrothermal methods are widely used because they offer easy control of reaction conditions and crystal morphology adjustment. However, hydrothermal methods often require long hydrothermal treatment times. For example, when using $AlCl_3$ as the raw material and ethylene glycol as the solvent, treatment for 6 h at 200 °C is necessary to obtain the pseudoboehmite crystalline form.[15] Pseudoboehmite can be prepared at a lower temperature using aluminum alkoxide hydrolysis; however, a strongly acidic solution is needed to promote particle dissolution,[16,17] which is potentially dangerous for adjuvant vaccine applications.

In this study, we developed an improved method to produce pseudoboehmite via the hydrolysis of aluminum alkoxide. Water and aluminum isopropoxide are the only raw materials, and baking or the addition of acid for dissolution is not required. Low hydrothermal temperatures and short times result in a milky-white colloid as the final product.

The obtained aluminum adjuvant has excellent suspension stability and good protein adsorption capacity. The hepatitis B virus surface antigen (HBsAg) was used as a model antigen to evaluate the efficacy of the adjuvant. A greater Th1 cellular immunity is induced by our adjuvant than by traditional aluminum adjuvants.

MATERIALS AND METHODS

Mice. Specific-pathogen-free (SPF) female mice (6−8 weeks old) were purchased from Beijing Vital River Laboratory Animal Technology Co., Ltd. (Beijing, China). They were kept in an SPF environment, and all animal experiments were approved by the Animal Ethics Committee of the National Vaccine and Serum Institute (Beijing, China).

Materials. Aluminum isopropoxide was purchased from Sigma-Aldrich (St. Louis, MO), Alhydrogel aluminum adjuvant was purchased from InvivoGen (San Diego, CA), and Alu-Gel-S aluminum adjuvant was purchased from SERVA Electrophoresis GmbH (Heidelberg, Germany). Aluminum adjuvant, prepared via the precipitation method, and HBsAg, produced under good manufacturing practice conditions, were provided by Beijing Tiantan Biological Products Corp., Ltd. (Beijing, China). A hepatitis B surface antibody (anti-HBs) enzyme-linked immunosorbent assay (ELISA) kit was purchased from Beijing Wantai Biological Pharmacy Enterprise Co., Ltd. (Beijing, China), and an IFN-γ secreting cell detection kit was purchased from Mabtech AB (Nacka Strand, Sweden). The HBsAg-specific cytotoxic T lymphocyte (CTL) polypeptide (12-mer S28−39 peptide "N"-IPQSLDSWWTSL−"C" of HBsAg) was synthesized by SBS Genetech Co., Ltd. (Beijing, China), and the HBsAg quantitative chemiluminescent immunoassay (CLIA) kit used for HBsAg quantification was purchased from Autobio Diagnostic Co., Ltd. (Zhenzhou, China).

Preparation of Aluminum Adjuvants by Hydrolysis. Aluminum isopropoxide (50 g) was added to toxoid-free water (500 mL), which was then heated with stirring, and the temperature was maintained at 60 °C to accelerate the volatilization of the isopropanol produced by the hydrolysis reaction. The mixture was stirred for 2 h and then left to stand before the supernatant was poured away after complete precipitation. A further 500 mL of water was injected, and the mixture was heated at 60 °C with stirring for 2 h and then left to stand before the supernatant was poured away. For the final step, two treatment methods were used as follows. For method 1, water (1000 mL) was injected to resuspend the mixture; the mixture was then sterilized at 120 °C for 30 min. For method 2, water (1000 mL) was injected to resuspend the mixture; it was mixed in a high-shear mixer at 10,000 rpm for 10 min and then subjected to three homogenization treatments at 800 bar. After homogenization, the sample was sterilized at 120 °C for 30 min.

Particle Size and ζ Potential Characterization. The aluminum content of the adjuvant was determined by inductively coupled plasma mass spectrometry (ICP-MS) after dilution with water to obtain a 0.5 mg/mL concentration, and the particle size and ζ potential were determined using a Zetasizer Nano ZS90 (Malvern Panalytical). Two commercial aluminum adjuvants (Alhydrogel and Alu-Gel-S) and an aluminum adjuvant prepared by precipitation were also analyzed via the same method.

XRD Analysis Characterization. An appropriate amount of aluminum adjuvant solution (total aluminum content, ≈200 mg) was centrifuged at 10,000g for 20 min, after which the supernatant was discarded, and the residual solid was resuspended in deionized water. This mixture was then centrifuged, the supernatant was discarded, then water was added to resuspend the residual solid, which was then centrifuged and washed; this process was repeated three times. The precipitate was then poured out, left to dry naturally, and then characterized by XRD (Shimadzu XRD-6100). The X-ray beam was generated using a Cu target; the tube voltage was 40 kV, and the current was 30 mA. The scan angle range was 5−80°.

Scanning Electron Microscopy (SEM) Characterization. The aluminum adjuvant sample was shaken evenly. Then, water was added to obtain a concentration of 1 mg/mL, and the diluted sample was dripped onto aluminum foil using a pipette before being left to dry naturally. After drying, the samples were observed using SEM (Zeiss Sigma 500).

Protein Adsorption by Aluminum Adjuvants—Adsorption Capacity Test. To observe the adsorption of proteins by the aluminum adjuvants, fluorescent proteins were used for testing. As examples, we selected two fluorescent proteins: green fluorescent protein (Clover) and red fluorescent protein (mRuby). The procedure was as follows: 5 mL of 0.1 mg/mL aluminum adjuvant and 5 mL of 0.4 mg/mL fluorescent protein (Clover or mRuby) were mixed thoroughly. Samples (500 μL) were acquired at different time points, centrifuged at 12,000 rpm for 5 min, and the supernatant was extracted. The protein content in the supernatant was the amount of free protein that had not been adsorbed by the aluminum adjuvant. The amount of adsorbed protein was calculated as the total protein amount minus the free amount. After the adsorption was saturated, the adsorption capacity of the aluminum adjuvant for the protein was calculated as the measured amount of adsorbed protein divided by the amount of the aluminum adjuvant. The

https://doi.org/10.1021/acsomega.2c04266
ACS Omega 2022, 7, 34528−34537

hydrolyzed aluminum used in this experiment was prepared using method 2.

Protein Adsorption by Aluminum Adjuvants—Adsorption Kinetics Curve. The aluminum adjuvant (0.5 mL, 0.1 mg/mL) and Clover (0.5 mL, 0.4 mg/mL) were mixed thoroughly. Samples (100 μL) were acquired at different time points and then filtered with a 200 nm pore-size filter to measure the concentration of the unadsorbed protein in the filtrate. The adsorbed protein amount was calculated as the difference between the total protein amount and the unadsorbed protein amount. The Clover adsorption kinetics curve of the aluminum adjuvant was plotted with time as the abscissa and protein adsorption capacity as the ordinate. The hydrolyzed aluminum used in this experiment was prepared using method 2.

Protein Adsorption by Aluminum Adjuvants—Suspension Stability Test. Each aluminum adjuvant (4 mL, 0.5 mg/mL) was added to a different 15 mL centrifuge tube along with Clover (1.5 mg), and the volume was made up to 5 mL with water. After thorough mixing, the tubes were positioned upright to allow natural sedimentation to occur. Clover deposition on the aluminum adjuvant could be clearly seen after adsorption. The corresponding scale (volume after sedimentation) at the upper edge of the aluminum adjuvant was observed and recorded every 15 min. The volume of the adjuvant after sedimentation was divided by the total volume, and this value was recorded as the suspension stability index. The hydrolyzed aluminum used in this experiment was prepared using method 2.

Antigen Adsorption Efficiency Stability Test. Equal volumes of aluminum adjuvant (0.5 mg/mL) and HBsAg (10 μg/mL) were mixed to prepare the vaccine. After thorough mixing, the solutions were placed at 4, or 37 °C for 7 d and then centrifuged at 12,000 rpm for 5 min. An HBsAg quantitative CLIA kit was used to detect the free antigen amount in the supernatant, and subsequently, the antigen adsorption rate was calculated ((total antigen amount − free antigen amount)/total antigen amount × 100%).

In Vivo Comparison of Different Aluminum Adjuvants. HBsAg was used to compare the efficacies of the four different aluminum adjuvants: the aluminum adjuvants prepared by hydrolysis and precipitation (referred to as "hydrolysis Al" and "precipitation Al," respectively, hereinafter) and the Alhydrogel and Alu-Gel-S commercial aluminum adjuvants. All of the immune samples were tested for endotoxin content using Limulus Reagent to ensure that their endotoxin content was less than 1 IU/mL.

Twenty-five BALB/c mice were randomly divided into five groups. The groups and treatments for each immune sample were as follows: HBsAg (0.5 μg) + 0.9% NaCl (control group), HBsAg (0.5 μg) + Alhydrogel (25 μg), HBsAg (0.5 μg) + Alu-Gel-S (25 μg), HBsAg (0.5 μg) + precipitation Al (25 μg), and HBsAg (0.5 μg) + hydrolysis Al (25 μg). The hydrolyzed aluminum used was prepared using method 2. The mice were immunized intramuscularly three times, at week 0, week 2, and week 4. Blood was collected at week 5, and antibody titers were measured by ELISA according to the kit instructions. In each case, the spleen was also taken, lymphocytes were separated, and the secretion of antigen-specific IFN-γ was detected by enzyme-linked immunospot (ELISPOT): 5×10^5 lymphocytes per well were seeded in 96-well plates (precoated with anti-IFN-γ monoclonal antibody). Subsequently, 200 μL of RPMI-1640 medium containing 10% fetal bovine serum, along with 0.5 μg of HBsAg S28−39 CTL peptide, was added to each well. After culturing for 18 h, the medium was discarded and 200 μL of phosphate-buffered saline was added to each well and washed five times. Then, the secondary antibody was added and incubated at 37 °C for 2 h. The plate was washed again, and the streptavidin−alkaline phosphatase conjugate was added to each well and incubated at room temperature for 1 h. Subsequently, the plate was washed and a chromogenic substrate (BCIP/NBT) was added to develop color; the reaction was terminated by washing with water. A CTL ImmunoSpot Analyzer (Cellular Technology Limited, Shaker Heights, Ohio) was used to detect the number of spots.

In Vivo Comparison of Effects of Different Hydrolyzed Aluminum Adjuvant Doses. Twenty BALB/c mice of 6−8 weeks were randomly divided into four groups. The aluminum adjuvant prepared by precipitation was used as the control, and the dose−response relationship of the aluminum adjuvant prepared by hydrolysis was examined. The groups and doses were as follows: HBsAg (0.5 μg) + precipitation Al (25 μg) (control group); HBsAg (0.5 μg) + hydrolysis Al (25 μg); HBsAg (0.5 μg) + hydrolysis Al (5 μg); and HBsAg (0.5 μg) + hydrolysis Al (1 μg).The hydrolyzed aluminum used in this experiment was prepared using method 2. Intramuscular immunization was performed three times, at 0, 2, and 4 weeks. Blood was collected at the fifth week, and after serum separation, the antibody titer was measured by ELISA according to the kit instructions. Simultaneously, the spleen was taken, lymphocytes were isolated, and antigen-specific cytokine secretion was measured by ELISPOT following the protocol mentioned previously.

Data Analysis. The data were analyzed using GraphPad Prism 8 software (GraphPad Prism Inc.), and the results were expressed as mean ± standard deviation ($x \pm SD$). One-way analysis of variance (ANOVA) was used for comparisons within groups, posthoc Tukey's test was used for multiple comparisons between groups, and *t*-tests were used for pairwise comparisons between groups. If $P < 0.05$, the data were considered to be significantly different. The protein adsorption curves of the aluminum adjuvants were fitted to the Michaelis−Menten equation, and the affinity of the different adjuvants for the proteins was compared using K_M values.

RESULTS

Aluminum Adjuvants Prepared by Hydrolysis Have Pseudoboehmite Structures. Aluminum hydroxide and aluminum phosphate are two commonly used aluminum adjuvants, and they are prepared via similar methods: two substances are left to mix and a precipitate is formed. For example, when preparing aluminum hydroxide, an aluminum salt (such as aluminum chloride, aluminum sulfate, or aluminum nitrate) is left to mix with an alkaline solution (such as sodium hydroxide, potassium hydroxide, or urea), during which time the reaction occurs and the precipitate is formed. Aluminum hydroxide adjuvants with different forms can be prepared by controlling the initial salt concentration, pH of the reaction solution, stirring speed, and reaction temperature.

We speculated that aluminum adjuvants obtained by different preparation methods could induce different adjuvant effects. To test this hypothesis, we used the hydrolysis method to prepare aluminum adjuvants with pseudoboehmite structures.

https://doi.org/10.1021/acsomega.2c04266
ACS Omega 2022, 7, 34528−34537

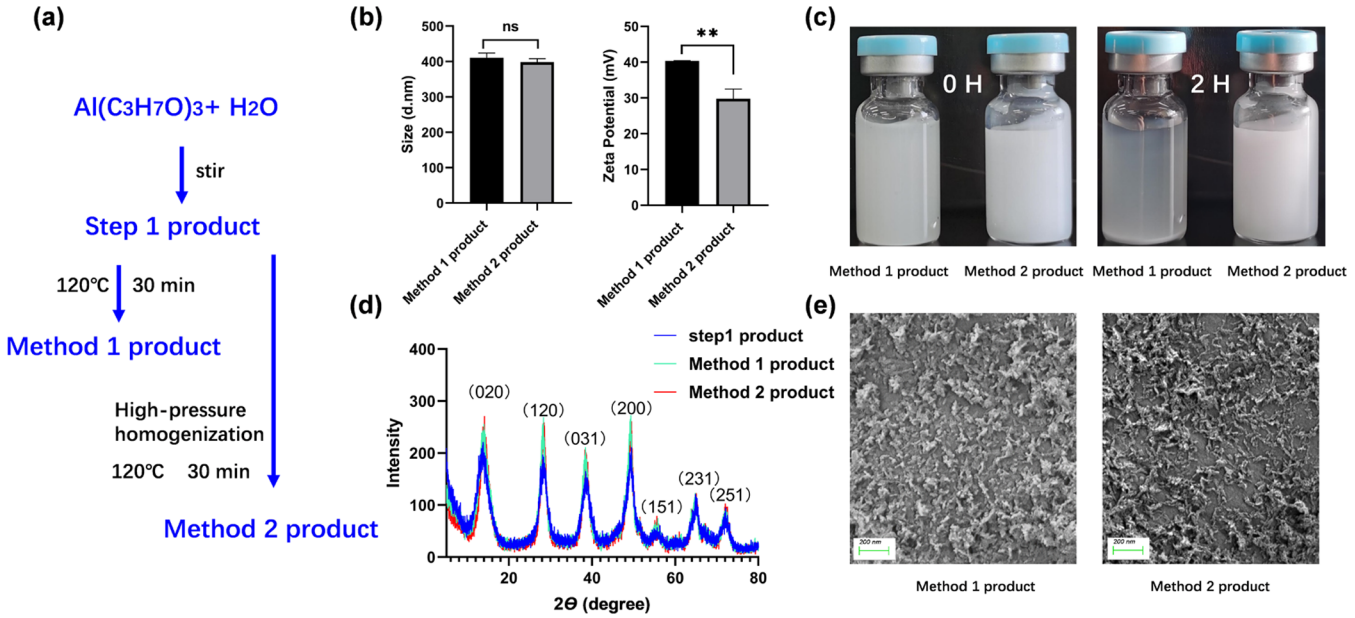

Figure 1. (a) Flow chart showing the method used for preparing aluminum adjuvants by hydrolysis in this study. (b) Comparison of particle sizes and ζ potentials of products prepared via methods 1 and 2. (c) Photographs illustrating the different sedimentation speeds of the method 1 and 2 products. (d) XRD analysis of intermediate and final products. (e) SEM images of aluminum adjuvants prepared using the two methods. The data in (b) are presented as mean ± SD (n = 3), and t-tests were used for comparisons between groups (**P < 0.01, ns means not significant).

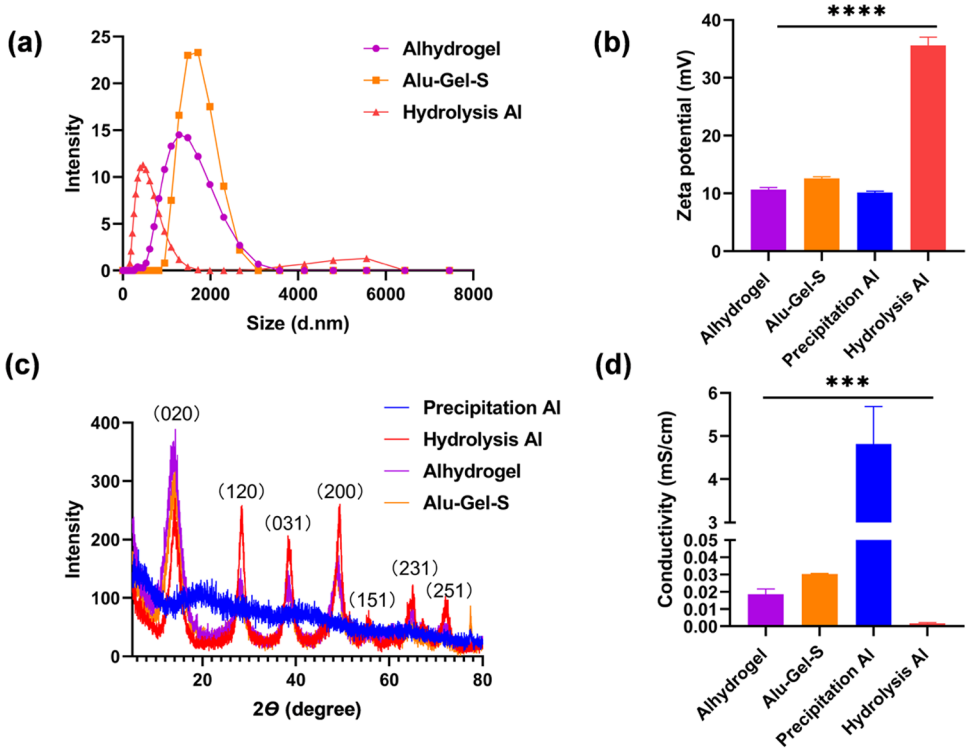

Figure 2. (a) Particle size distributions, (b) ζ potentials, (c) XRD patterns, and (d) conductivities of Alhydrogel, Alu-Gel-S, and aluminum adjuvants prepared via hydrolysis and precipitation. The data in (b) and (d) are presented as mean ± SD (n = 2). For data analysis, one-way ANOVA was used for multiple comparisons within groups (***P < 0.001, ****P < 0.0001).

We explored the influence of different treatments after aluminum isopropanol hydrolysis, before high-temperature sterilization. As shown in Figure 1, two methods were compared: direct sterilization (method 1) and high-pressure homogenization before high-temperature sterilization (method 2). It was observed that the particles in the samples obtained via method 1 rapidly sank after they were suspended; however, the samples obtained via method 2 remained within a translucent gelatinous liquid, and no obvious subsidence was observed after long periods (Figure 1c). Dynamic light scattering showed that the particle size for the samples obtained via method 2 was smaller than that of the samples obtained by method 1 (Figure 1b). However, the difference between them was not significant (P > 0.05), and they had

https://doi.org/10.1021/acsomega.2c04266
ACS Omega 2022, 7, 34528−34537

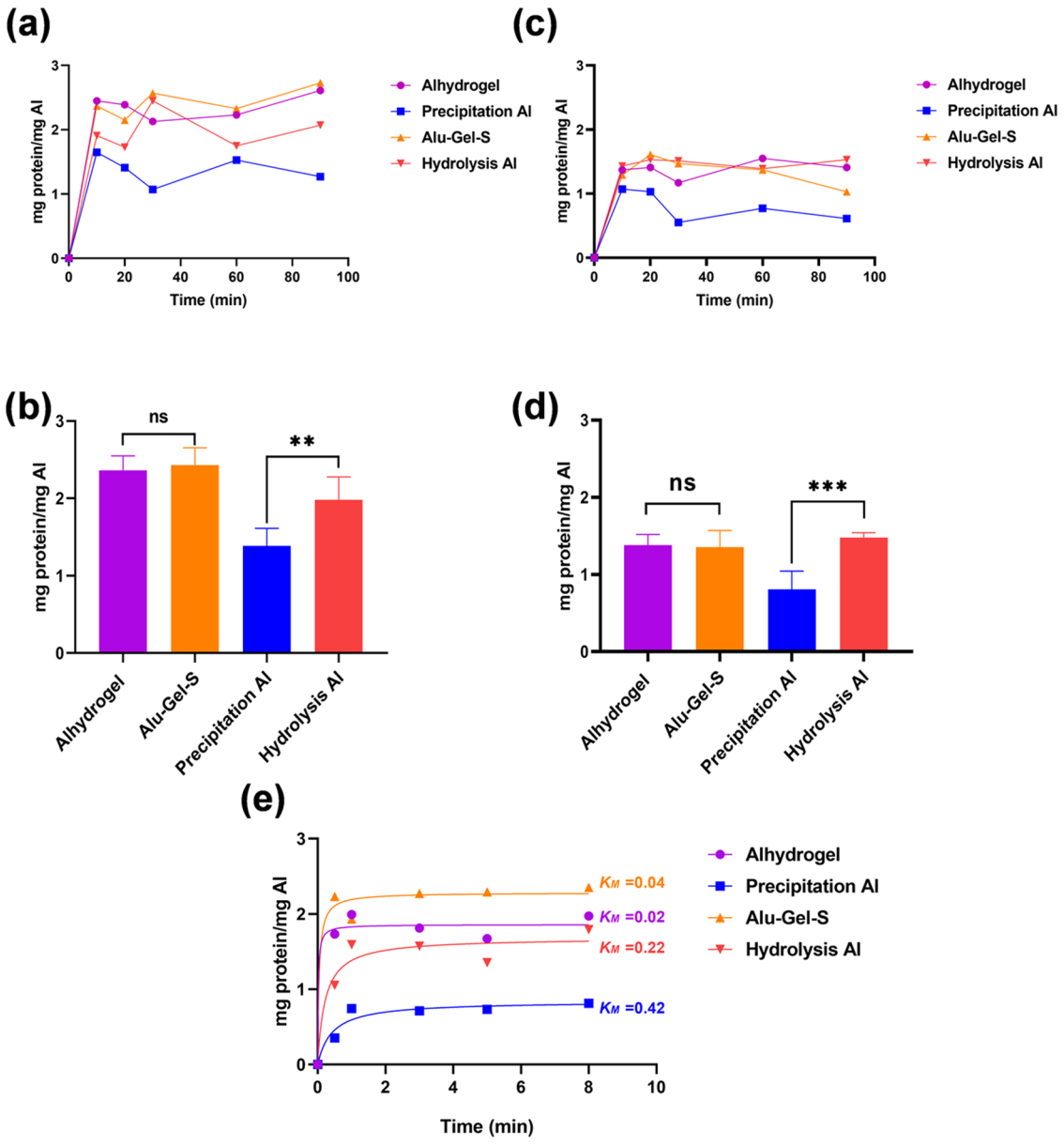

Figure 3. (a) Clover and (c) mRuby adsorption curves of various aluminum adjuvants. Adsorption capacities of various aluminum adjuvants for (b) Clover and (d) mRuby. (e) Kinetics of adsorption of Clover by various aluminum adjuvants and the corresponding K_M values. The data in (b) and (d) are presented as mean ± SD (n = 5), and t-tests were used for comparisons between groups (**P < 0.01, ***P < 0.001, ns means not significant).

almost the same appearance in electron microscopy images (Figure 1e), excluding the difference in particle size and morphology that led to the difference in the sedimentation rate of the two adjuvants. The ζ potential (Figure 1b) of the homogenized samples (method 2) was significantly smaller than that of the unhomogenized samples (method 1). This result is not in accordance with the conventional understanding that the greater the absolute value of the ζ potential, the more stable the particle, indicating that the factors that influence particle stability are more complex in this case.

XRD analysis was performed on the as-hydrolyzed samples and the samples obtained by method 1 and method 2 (Figure 1d); in each case, diffraction peaks characteristic of pseudoboehmite were observed. Comparing the 2θ values for the (020) diffraction peaks in the different samples, for the as-hydrolyzed sample, this value was 13.54°, whereas it was 13.86° after the method 1 treatment and 14.14° after the method 2 treatment. The (020) diffraction peak intensities of the three samples gradually increased in order step 1 (204) < method 1 (226) < method 2 (270), and it was apparent that the product obtained via method 2 had the best crystallinity. Compared with conventional boehmite preparation methods, which require higher hydrothermal temperatures and longer times, in this study, we developed a simple method for obtaining the pseudoboehmite aluminum adjuvant in the form of a stable colloid. We optimized the technological process of preparing aluminum adjuvant by hydrolysis via aluminum isopropanol hydrolysis, elutriation, homogenization, and finally high-temperature sterilization. The hydrolyzed aluminum used in subsequent experiments (characterization, protein adsorption capacity, suspension stability, and in vivo adjuvant effect test) was prepared using method 2.

https://doi.org/10.1021/acsomega.2c04266
ACS Omega 2022, 7, 34528−34537

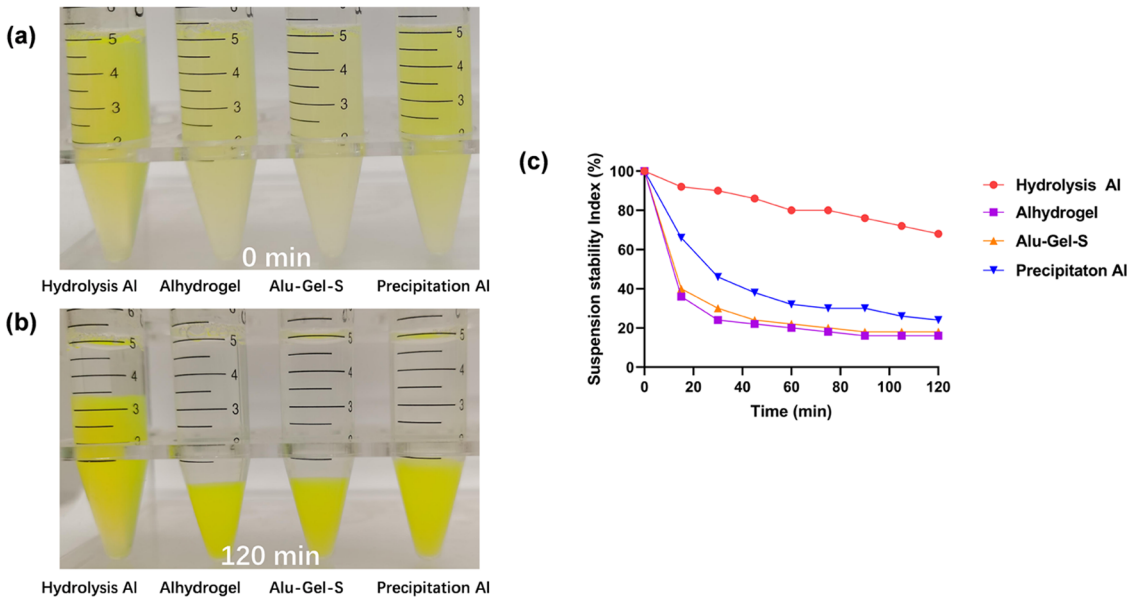

Figure 4. Suspension stabilities of aluminum adjuvants. Photographs showing the suspensions at (a) 0 min and (b) 120 min after the aluminum adjuvant was mixed with Clover protein. (c) Suspension stability indices of aluminum adjuvants vs time.

Particle Sizes, ζ Potentials, and XRD Patterns of Various Aluminum Adjuvants. The aluminum adjuvant samples were diluted to the same concentration, and the particle sizes and ζ potentials were measured (Figure 2). The aluminum adjuvant prepared by hydrolysis (hydrolysis Al, prepared by method 2) had the smallest particles (Figure 2a), and its ζ potential was much larger than those of the other three aluminum adjuvants (Figure 2b). The particle size of the sample prepared by precipitation (precipitation Al) was extremely large and exceeded the detection limit of the machine, so it is not included in Figure 2a.

However, because hydrolysis Al was dispersed in pure water in this study, it had very low conductivity, similar to the conductivities of the Alhydrogel and Alu-Gel-S aluminum adjuvants and far lower than that of the precipitation Al sample (Figure 2d), which was dispersed in sodium chloride solution. Because the hydrolysis Al solution is only water, when the adjuvant is mixed with an antigen, the solution, unlike the buffer, has little effect on the antigen.

XRD analysis was performed on the different aluminum adjuvant samples (Figure 2c). Alhydrogel and Alu-Gel-S were found to have XRD spectra similar to that of the hydrolysis Al sample prepared in this study. However, slight differences between the diffraction peaks were observed (Figure 2c). The (020) diffraction peaks of Alhydrogel and Alu-Gel-S are more intense than those of hydrolysis Al, whereas the other diffraction peaks are less intense, indicating that the crystal structures are not identical. The XRD pattern of the precipitation Al sample is completely different from those of the other aluminum adjuvant samples.

Aluminum Adjuvants Prepared by Hydrolysis Have Good Protein Adsorption Capacity. To facilitate observation, fluorescent proteins were used to evaluate the adsorption capacities of the aluminum adjuvants. The amounts of protein adsorbed by the different aluminum adjuvants were measured, and the adsorption capacities of the aluminum adjuvants were calculated.

Figure 3 shows that various aluminum adjuvants with pseudoboehmite structures had good adsorption capacity for the two tested fluorescent proteins: the amounts of Clover adsorbed per milligram of Alhydrogel, Alu-Gel-S, and hydrolysis Al (prepared by method 2) were approximately 2.4, 2.4, and 2.0 mg, respectively, whereas the amount of Clover adsorbed per milligram of precipitation Al was only approximately 1.4 mg. The amounts of mRuby protein adsorbed per milligram of Alhydrogel, Alu-Gel-S, and hydrolysis Al were approximately 1.3, 1.4, and 1.5 mg, respectively, whereas the amount adsorbed by precipitation Al was only approximately 0.8 mg. Thus, the hydrolysis Al sample prepared in this study had excellent protein adsorption capacity. Previous studies have suggested that the width at half-height (WHH) of the (020) diffraction band of pseudoboehmite is related to its capacity to adsorb proteins, with a larger WHH indicating a better protein adsorption capacity.[18] Our results showed that there is no absolute correlation between this XRD analysis parameter and the protein adsorption capacity, and the adsorption capacity results may be different for different proteins. Alhydrogel had the greatest WHH for the (020) peak, but among the three pseudoboehmite aluminum adjuvants, it had the smallest adsorption capacity for the mRuby protein.

We also plotted the Clover adsorption kinetics curves of the different aluminum adjuvants (Figure 3e). The figure shows that the adsorption by the different aluminum adjuvants of the protein is very rapid (equilibrium is reached within 2 min), and the aluminum adjuvants with pseudoboehmite structure have smaller K_M values, indicating that they have stronger affinities for proteins. The equilibrium adsorption values are a little different from the protein adsorption capacities (Figure 3b) because a filter membrane was used to stop the adsorption of aluminum to obtain the data shown in Figure 3e, and the filter membrane would have adsorbed some protein.

In conclusion, the obtained results show that the adsorption capacity and adsorption speed of the aluminum adjuvants with pseudoboehmite structures are greater than those with precipitation Al (the XRD pattern of which is completely different from that of pseudoboehmite).

https://doi.org/10.1021/acsomega.2c04266
ACS Omega 2022, 7, 34528−34537

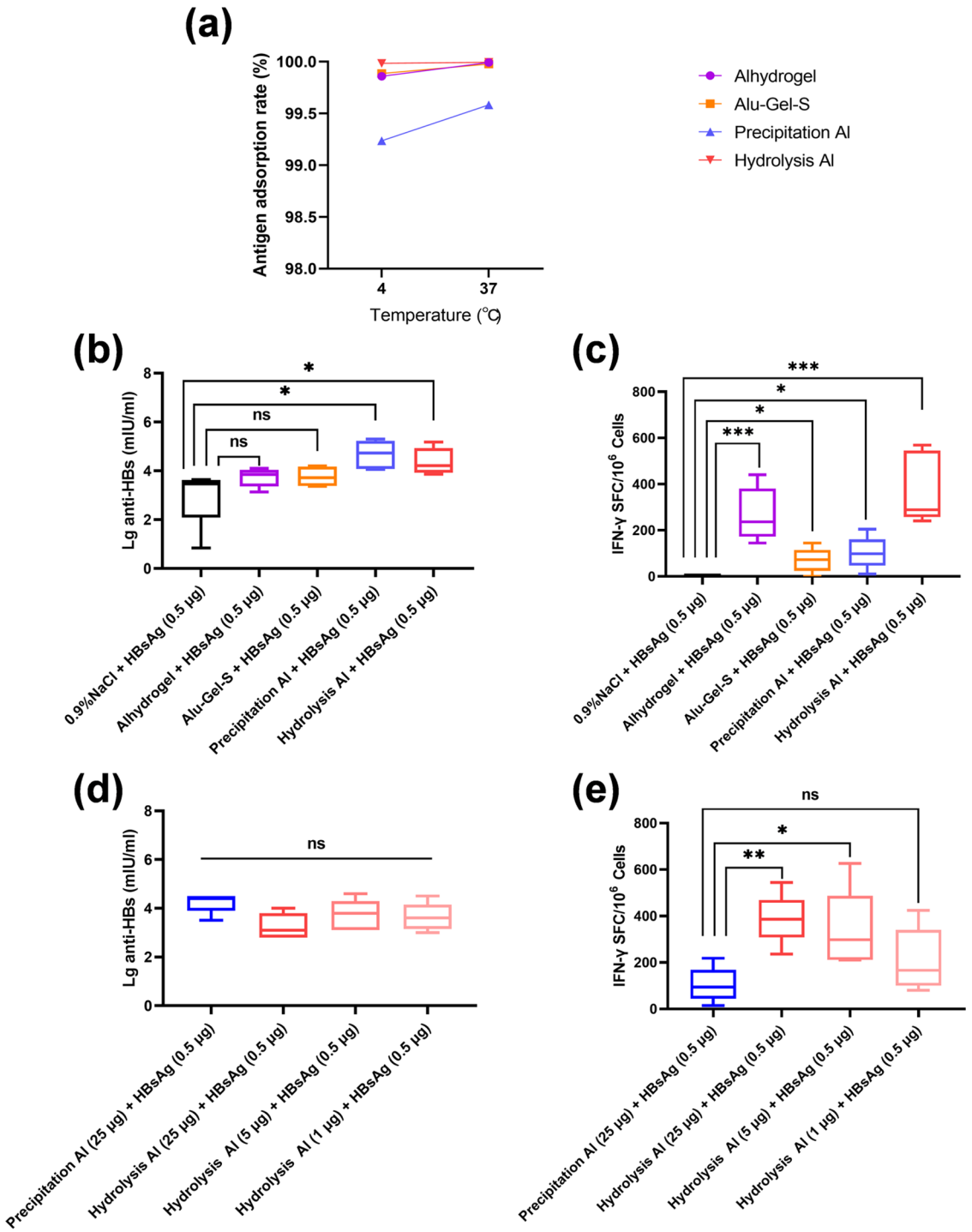

Figure 5. Antigen adsorption efficiency stability of different aluminum adjuvants and the in vivo efficacy of the adjuvant using HBsAg as a model antigen. (a) Adsorption efficiency stability. (b) Antibody titers and (c) antigen-specific IFN-γ secretion levels after immunization with different adjuvants using the same dose. (d) Antibody titers and (e) antigen-specific IFN-γ secretion levels after immunization with different doses of the adjuvant prepared by hydrolysis. Data are presented as mean ± SD (n = 5), and t-tests were used for comparisons between groups (*P < 0.05, **P < 0.01, ***P < 0.0005, ns means not significant).

Hydrolyzed Aluminum Adjuvants Have Excellent Suspension Stability. The prepared aluminum adjuvant was mixed with the antigen and then divided into separate doses before packaging. This process often requires adequate mixing to avoid differences in the immunological effectiveness of the same vaccine batch due to rapid sedimentation of aluminum adjuvants affecting product homogeneity. Better suspension stability for an aluminum adjuvant is advantageous in terms of product uniformity. In this study, we mixed different aluminum adjuvants with fluorescent proteins using the same amounts and then observed the sedimentation of the adjuvant (Figure 4). The aluminum adjuvant prepared by precipitation and the two commercially available aluminum adjuvants settled rapidly after mixing (50% settled within 40 min and 80% within 120 min). However, the aluminum adjuvant prepared by hydrolysis in this study exhibited

https://doi.org/10.1021/acsomega.2c04266
ACS Omega 2022, 7, 34528−34537

excellent suspension stability (only 30% settled within 120 min). Better suspension stability (a fluffier structure) is conducive to more uniform adsorption of an antigen after mixing.

Hydrolyzed Aluminum Adjuvants Can Induce Stronger Th1 Cellular Immunity. Based on their self-assembled form, recombinant antigens can be divided into two categories: viruslike particles (VLPs) and non-VLPs. The VLPs have a viruslike particle structure, and they tend to have better immunogenicity. Currently, a majority of the approved hepatitis B and HPV vaccines are VLP-based vaccines, and aluminum adjuvants are often used in these vaccines. In this study, HBsAg VLP was used as the model antigen to evaluate the adjuvant effect of hydrolysis Al and other aluminum adjuvants in mice. According to European Pharmacopoeia, the maximum limit for aluminum adjuvants in human vaccines is 1.25 mg/dose. In our study, the content of aluminum adjuvant used for immunization of mice was only 25 μg/dose (equivalent to 1/50 of the upper limit of the human dose).

The HBsAg with the VLP structure is extremely stable. The antigen content did not change significantly even when it was placed at a high temperature of 37 °C for 7 days (4 °C, 7 days: 5.24 ± 0.05 μg/mL; 37 °C, 7 days: 5.18 ± 0.35 μg/mL). Meanwhile, the results of the vaccine stability test show that various aluminum adjuvants used in animal experiments can effectively adsorb antigens and maintain long-term stability (Figure 5a).

After immunization, the group immunized with the antigen alone (control group) exhibited excellent antibody titers. There was no significant difference between the antibody titers of the groups immunized with the two commercial aluminum adjuvants compared with the control group, but the average antibody titer value of the adjuvant group was higher than that of the unadjuvanted group (Figure 5b). Nonetheless, precipitation Al and hydrolysis Al induced significantly stronger humoral immunity (Figure 5b).

The Th1 cellular immune responses induced by the adjuvants in each group were also analyzed (Figure 5c). There were almost no antigen-specific IFN-γ secreting cells detected among the lymphocytes isolated after immunization with the antigen alone, indicating that Th1 cellular immunity was inevitably correlated with humoral immunity. Both Alu-Gel-S and precipitation Al induced extremely weak Th1 cellular immunity, much weaker than that induced by Alhydrogel. As both Alhydrogel and Alu-Gel-S have similar pseudoboehmite structures, this result indicates that Th1 cellular immunity is not necessarily related to the pseudoboehmite structure of the aluminum adjuvant. Furthermore, remarkably, the hydrolysis Al we prepared elicited the strongest Th1 cellular immune response, which is of great significance for efforts to improve the protective effects of vaccines.

Owing to the complexity of the immune process, unlike chemical drugs with a single target, vaccines have a more complex dose−response relationship. In a follow-up experiment, we selected precipitation Al, which could induce the strongest humoral immunity, as the control, and we compared the adjuvant effects of different doses of hydrolysis Al using HBsAg (Figure 5d). The level of humoral immunity induced by hydrolysis Al was not significantly correlated with the adjuvant dose. The humoral immunity induced by hydrolysis Al at doses in the range of 1−25 μg was comparable to that induced by a dose of 25 μg of precipitation Al, and the difference between the groups was not significant. These results again demonstrate the excellent ability of hydrolysis Al to induce humoral immunity. Moreover, Figure 5e shows that the level of Th1 cellular immunity induced by hydrolysis Al is much higher than that induced by the aluminum adjuvant prepared by the traditional precipitation method (precipitation Al); even when the hydrolysis Al dosage is only one-fifth of the precipitation Al dosage, the Th1 cellular immune response is still significantly stronger. This capacity to induce a Th1 cellular immune response correlates with the hydrolysis Al dose. Based on these observed results, we speculate that when using HBsAg as the antigen, the optimal ratio of hydrolysis Al to the antigen mass is greater than or equal to 10:1. Compared with the precipitation Al, when the content of aluminum adjuvant is the same, the antigen content can be reduced by up to 4/5; when the antigen content is the same, the amount of aluminum adjuvant added can be reduced by up to 4/5.

DISCUSSION

As the oldest and most widely used adjuvants, aluminum adjuvants have been recognized for their safety and are capable of eliciting a good humoral immune response; however, the lack of Th1 cellular immunity induction has long been recognized as a shortcoming. A common approach to strengthening the cellular immune responses generated by aluminum adjuvants is to combine an aluminum adjuvant with an immunostimulatory agent. For example, AS04[19] (aluminum combined with TLR4 agonist 3-O-deacyl-4′-monophosphoryl Lipid A (MPLA)) is used for HPV vaccines,[20] alum is combined with a TLR9 agonist (CpG) in a COVID-19 vaccine[21] and in a smallpox subunit vaccine,[22] and aluminum adjuvants are combined with STING agonist 2′3′-cGMAP in recombinant hemagglutinin (rHA) influenza vaccine.[23]

Another method is to reduce the particle size of the aluminum adjuvant so that it can enter lymph nodes with more CD8 lymphocytes, thereby directly stimulating CD8, which can theoretically improve the level of Th1 cellular immunity.[24] For example, a nanosized aluminum hydroxide adjuvant has been combined with the immunostimulatory CpG as a delivery carrier, and this enabled it to effectively target lymph nodes to better stimulate immune cells and induce stronger cellular immune responses.[25]

In contrast to the aforementioned two methods, in this study, to evaluate the hypothesis that the adjuvant properties of aluminum can be altered by changing its morphology, we used a new strategy to prepare aluminum adjuvants via hydrolysis. The aluminum adjuvant we prepared in this study has a pseudoboehmite structure. It has excellent antigen adsorption capacity. Our results also showed that although an advantage of the pseudoboehmite structure was its protein adsorption capacity, this structure was not necessarily related to the adjuvant effect. Unlike previously reported pseudoboehmite preparation methods, which require high temperatures and long durations for hydrothermal synthesis, the improved method developed in this study is rapid, and the reaction proceeds at low temperatures. The new method also has the advantage of simple preparation conditions. In addition, the obtained aluminum adjuvant has good suspension stability, and when it is used for preparing aluminum-adsorbed vaccines, this property should lead to improvements in the homogeneity of the final product.

The results of subsequent animal experiments using HBsAg as a model antigen showed that the new preparation method

https://doi.org/10.1021/acsomega.2c04266
ACS Omega 2022, 7, 34528−34537

yields an aluminum adjuvant with the capacity to induce a significantly stronger cellular immune response, without the requirement of an immunostimulatory agent, as well as a strong humoral immune response. Hence, our new method is of great significance for the development of vaccines that exhibit improved protective effects.

In conclusion, by tuning an aluminum adjuvant preparation method, we obtained an aluminum adjuvant with different physicochemical properties and appearances, and its adjuvant effect was also improved. Aluminum adjuvants have often been regarded as simple systems, but we still do not have a complete understanding of this material and its bioactivity. Some conclusions of previous studies on the mechanism of aluminum adjuvant are contradictory, which suggests that the mechanism of aluminum adjuvant action is complex. Although the results of our study prove that the different physical and chemical properties can yield different effects, the biological effects obtained due to different physical and chemical properties are very complex. Unfortunately, in this study, we could not determine the reason for the strong Th1 cellular immunity induced by hydrolyzed aluminum. We believe that the data produced by this study provides a good reference point for future efforts aimed at obtaining aluminum adjuvants with even better properties.

AUTHOR INFORMATION

Corresponding Author

Jing Xu − *National Vaccine and Serum Institute, Beijing 101111, China*; Email: xj17b@163.com, xujing13@sinopharm.com

Authors

Zhibiao Wang − *National Vaccine and Serum Institute, Beijing 101111, China*; orcid.org/0000-0001-6068-3737

Shuxiang Li − *National Vaccine and Serum Institute, Beijing 101111, China*

Pu Shan − *National Vaccine and Serum Institute, Beijing 101111, China*

Duoqian Wei − *National Vaccine and Serum Institute, Beijing 101111, China*

Shaojie Hao − *National Vaccine and Serum Institute, Beijing 101111, China*

Zhuan Zhang − *National Vaccine and Serum Institute, Beijing 101111, China*

Complete contact information is available at: https://pubs.acs.org/10.1021/acsomega.2c04266

Author Contributions

The manuscript was written through the contribution of all authors. Z.W. performed adjuvant preparation, characterization, and protein adsorption evaluation; Z.W., S.L., P.S., D.W., and S.H. performed the in vivo evaluation; Z.W. conceived the project and wrote the manuscript; J.X. supervised and directed the project. All authors discussed the results and commented on the manuscript. All authors have given approval to the final version of the manuscript.

Notes

The authors declare no competing financial interest.

ACKNOWLEDGMENTS

This work was financially supported by the National Science and Technology Key Project on Major Infectious Diseases (grant no. 2017ZX10202201-002-002).

REFERENCES

(1) Glenny, A. T.; Pope, C. G.; Waddington, H.; Wallace, U. Immunology Notes. XXIII. The antigenic value of toxoid precipitated by potassium alum. *J. Pathol. Bacteriol.* **1926**, 31−40.

(2) Marrack, P.; McKee, A. S.; Munks, M. W. Towards an understanding of the adjuvant action of aluminium. *Nat. Rev. Immunol.* **2009**, *9*, 287−293.

(3) Colaprico, A.; Senesi, S.; Ferlicca, F.; Brunelli, B.; Ugozzoli, M.; Pallaoro, M.; O'Hagan, D. T. Adsorption onto aluminum hydroxide adjuvant protects antigens from degradation. *Vaccine* **2020**, *38*, 3600−3609.

(4) Li, H.; Nookala, S.; Re, F. Aluminum hydroxide adjuvants activate caspase-1 and induce IL-1β and IL-18 release. *J. Immunol.* **2007**, *178*, 5271−5276.

(5) Hornung, V.; Bauernfeind, F.; Halle, A.; Samstad, E. O.; Kono, H.; Rock, K. L.; Fitzgerald, K. A.; Latz, E. Silica crystals and aluminum salts activate the NALP3 inflammasome through phagosomal destabilization. *Nat. Immunol.* **2008**, *9*, 847−856.

(6) Hutchison, S.; Benson, R. A.; Gibson, V. B.; Pollock, A. H.; Garside, P.; Brewer, J. M. Antigen depot is not required for alum adjuvanticity. *FASEB J.* **2012**, *26*, 1272−1279.

(7) de Veer, M.; Kemp, J.; Chatelier, J.; Elhay, M. J.; Meeusen, E. N. T. The kinetics of soluble and particulate antigen trafficking in the afferent lymph, and its modulation by aluminum-based adjuvant. *Vaccine* **2010**, *28*, 6597−6602.

(8) Wu, J.; Ma, G. Imitation of nature: Bionic design in the study of particle adjuvants. *J. Controlled Release* **2019**, *303*, 101−108.

(9) Xu, L.; Wang, X.; Wang, W.; Sun, M.; Choi, W. J.; Kim, J.-Y.; Hao, C.; Li, S.; Qu, A.; Lu, M.; Wu, X.; Colombari, F. M.; Gomes, W. R.; Blanco, A. L.; de Moura, A. F.; Guo, X.; Kuang, H.; Kotov, N. A.; Xu, C. Enantiomer-dependent immunological response to chiral nanoparticles. *Nature* **2022**, *601*, 366−373.

(10) Fitzgerald, J. J.; Piedra, G.; Dec, S. F.; Seger, M.; Maciel, G. E. Dehydration studies of a high-surface-area alumina (pseudo-boehmite) using solid-state 1H and 27Al NMR. *J. Am. Chem. Soc.* **1997**, *119*, 7832−7842.

(11) Zhang, L.; Cheng, B.; Shi, W.; Samulski, E. T. In-situ electrochemical synthesis of 1-dimensional alumina nanostructures. *J. Mater. Chem.* **2005**, *15*, 4889−4893.

(12) Proost, J.; Boxel, S. V. Large-scale synthesis of high-purity, one-dimensional α-Al2O3 structures. *J. Mater. Chem.* **2004**, *14*, 3058−3062.

(13) Ghosh, S.; Naskar, M. K. Synthesis of mesoporous γ-alumina nanorods using a double surfactant system by reverse microemulsion process. *RSC Adv.* **2013**, *3*, 4207−4211.

(14) Vitorino, N. M. D.; Kovalevsky, A. V.; Abrantes, J. C. C.; Frade, J. R. Hydrothermal synthesis of boehmite in cellular alumina monoliths for catalytic and separation applications. *J. Eur. Ceram. Soc.* **2015**, *35*, 3119−3125.

(15) Ma, M.-G.; Zhu, J.-F. A facile solvothermal route to synthesis of γ-alumina with bundle-like and flower-like morphologies. *Mater. Lett.* **2009**, *63*, 881−883.

(16) Padmaja, P.; Pillai, P. K.; Warrier, K. G. K.; Padmanabhan, M. Adsorption isotherm and pore characteristics of nano alumina derived from sol-gel boehmite. *J. Porous Mater.* **2004**, *11*, 147−155.

(17) Naseer, D.; Ha, J.-H.; Lee, J.; Park, C.; Song, I.-H. Effect of the peptization process and thermal treatment on the sol-gel preparation of mesoporous α-alumina membranes. *Membranes* **2022**, *12*, 313.

(18) Masood, H.; White, J. L.; Hem, S. L. Relationship between protein adsorptive capacity and the x-ray diffraction pattern of aluminium hydroxide adjuvants. *Vaccine* **1994**, *12*, 187−189.

(19) Garçon, N.; Van Mechelen, M.; Wettendorff, M. 10 - Development and evaluation of AS04, a novel and improved adjuvant

https://doi.org/10.1021/acsomega.2c04266
ACS Omega 2022, 7, 34528−34537

system containing MPL and aluminum salt. In *Immunopotentiators in Modern Vaccines* Schijns, V. E. J. C.; O'Hagan, D. T., Eds.; Academic Press: London, 2006; pp 161−177.
(20) Garçon, N.; Morel, S.; Didierlaurent, A.; Descamps, D.; Wettendorff, M.; Van Mechelen, M. Development of an AS04-adjuvanted HPV vaccine with the adjuvant system approach. *BioDrugs* **2011**, *25*, 217−226.
(21) Kuo, T.-Y.; Lin, M.-Y.; Coffman, R. L.; Campbell, J. D.; Traquina, P.; Lin, Y.-J.; Liu, L. T.-C.; Cheng, J.; Wu, Y.-C.; Wu, C.-C.; Tang, W.-H.; Huang, C.-G.; Tsao, K.-C.; Chen, C. Development of CpG-adjuvanted stable prefusion SARS-CoV-2 spike antigen as a subunit vaccine against COVID-19. *Sci. Rep.* **2020**, *10*, No. 20085.
(22) Xiao, Y.; Zeng, Y.; Schante, C.; Joshi, S. B.; Buchman, G. W.; Volkin, D. B.; Middaugh, C. R.; Isaacs, S. N. Short-term and longer-term protective immune responses generated by subunit vaccination with smallpox A33, B5, L1 or A27 proteins adjuvanted with aluminum hydroxide and CpG in mice challenged with vaccinia virus. *Vaccine* **2020**, *38*, 6007−6018.
(23) Borriello, F.; Pietrasanta, C.; Lai, J. C. Y.; Walsh, L. M.; Sharma, P.; O'Driscoll, D. N.; Ramirez, J.; Brightman, S.; Pugni, L.; Mosca, F.; Burkhart, D. J.; Dowling, D. J.; Levy, O. Identification and characterization of stimulator of interferon genes as a robust adjuvant target for early life immunization. *Front. Immunol.* **2017**, *8*, No. 1772.
(24) Fifis, T.; Gamvrellis, A.; Crimeen-Irwin, B.; Pietersz, G. A.; Li, J.; Mottram, P. L.; Mckenzie, I. F. C.; Plebanski, M. J. J. o. I. Size-dependent immunogenicity: therapeutic and protective properties of nano-vaccines against tumors. *J. Immunol.* **2004**, *173*, 3148−3154.
(25) Jiang, H.; Wang, Q.; Li, L.; Zeng, Q.; Li, H.; Gong, T.; Zhang, Z.; Sun, X. Turning the old adjuvant from gel to nanoparticles to amplify CD8+ T cell responses. *Adv. Sci.* **2018**, *5*, No. 1700426.

https://doi.org/10.1021/acsomega.2c04266
ACS Omega 2022, 7, 34528−34537